IMMERSION TYPE MULTI-CHANNEL AE SENSORS FOR CORROSION MONITORING OF UNDERGROUND FUEL TANK

Takuma Matsuo, Hideo Cho and Mikio Takemoto
Faculty of Science and Engineering, Aoyama Gakuin University,
5-10-1, Fuchinobe Sagamihara, Kanagawa 229-8558, Japan.

Abstract

Immersion-type AE sensor is needed for corrosion monitoring of underground gasoline tanks. We are developing a multi-directional optical fiber AE sensor to monitor the longitudinal AE signal through liquid (liquid-borne AE). The developed AE system is an optical-fiber-based Mach-Zender-type laser interferometer using a weak laser and is intrinsically safe. Multi-sensing function was facilitated by winding an optical fiber on four small-size short cup-shaped pipes with different diameters, which were installed on the inside walls of a box of 22.5-mm square and 230-mm height. Each sensor element was screwed on a different sidewall. The four fiber sensors were cascaded in series on a single fiber and monitored the liquid-borne AE signals from four directions simultaneously via frequency discrimination. As the each fiber-wound sensor element monitors at the resonant frequency of the pipe, we can estimate the direction of AE signals using their frequency spectra and wavelet transform. The functionality of the sensor was demonstrated by two month monitoring of liquid-borne AE signals from rust fractures on corroded four carbon steel sidewalls of a water tank. The immersion-type sensor successfully monitored liquid-borne AE signals from the four corroded plates. AE hit rates were considered to relate the corrosion of metallic pieces included in the rust, but not the corrosion of the substrate steel.

Keywords: Optical fiber AE sensor, intrinsically safe sensor, immersion type sensor, multi-channel sensor, environment adaptive system, rust fracture

Introduction

Integrity loss of underground fuel tanks by localized soil corrosion is becoming serious problems in Japan. Fire and Disaster Management Agency (FDMA) in Japan reports leak accidents of 344 tanks in 2001. Thirty percent of them were supposed to be caused by localized corrosion [1].

AE technique is expected to be a useful tool for monitoring corrosion damages of the tank, however we can not use the conventional AE system using the piezo-sensors, since the system is not intrinsically safe.

We are developing an optical fiber laser interferometer to monitor AE signals [2]. This system is intrinsically safe and previously used to monitor the liquid borne P-wave by immersing the sensing fiber into the liquid [3]. Here, a single sensing fiber was spirally wound on the pipe, and detected AE signals from any directions. We have improved this sensor as it can monitor the corrosion zone or the direction of the P-wave for long times.

We first introduce our new four direction AE sensor and next AE monitoring from four plates with rusts (corroded samples) for 50 days. We discuss relationship between AE activity and corrosion of the steel with rusts.

Immersion Type Optical Fiber Sensor

A sensing box developed is shown in Fig. 1. The box was designed for underground gasoline tanks with a 32 mm nozzle, and contains four AE sensors in its. Box size is 22.5 mm square and 230 mm height. Both the top and bottom of the box were rigidly fixed to thick plug plates, but four side walls of 1 mm thick aluminum plate were screwed to four 5 mm rectangular bars after inserting a special polymer sheet of 1 mm thickness. This structure can prevent the vibration interference of neighbor walls and the leak of gasoline into the box. A hollow long pipe of 16 mm diameter was screwed in the top plug plate. This pipe is used to insert the sensing box in the tank through a 32 mm diameter nozzle, and to connect the optical fiber to the monitoring system.

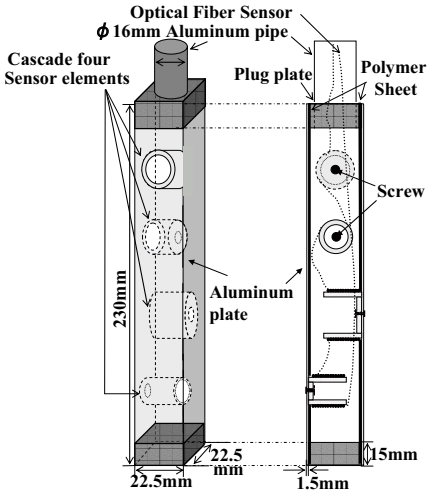

Fig.1 Immersion type four direction AE sensor using optical fiber

Sensing fiber was wound on four cap-shaped aluminum pipes of 20 mm height (called as the sensor element) with different diameters (12.5, 15, 18 and 19 mm). These elements were screwed on the side walls inserting the polymer sheet. The sensing fiber was wound on the holders multiple times. This structure improves the sensor sensitivity significantly. Four sensors were connected by a single fiber in a cascade manner and connected to the monitoring system via fiber connectors. Thus the four sensors detect the wall vibration excited by the liquid-borne P-wave. Here the different resonance frequencies of four sensors are successfully utilized to identify the direction of the P-wave. We call the sensor with 15 mm diameters element as "D15 sensor" and the system as ITFDS (Immersion Type Four Directional System), hereafter.

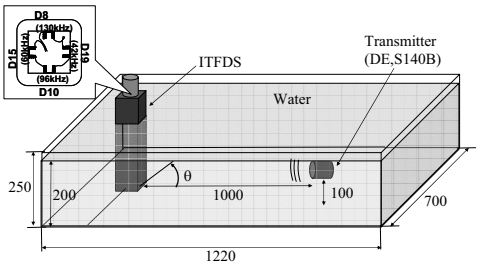

Fig.2 Experimental setup to study the directivity of the ITFDS

We first studied the directionality of the sensors to the water born P-wave using a water container with 1220 mm length, 700 mm width and 25 mm depth, as shown in Fig.2. We excited the water born P-wave using a PZT transmitter (resonance frequency 0f 140 kHz) immersed in water. We fixed the transmitter and rotated the sensing box in the counter clock wise. Figure 3 show examples of

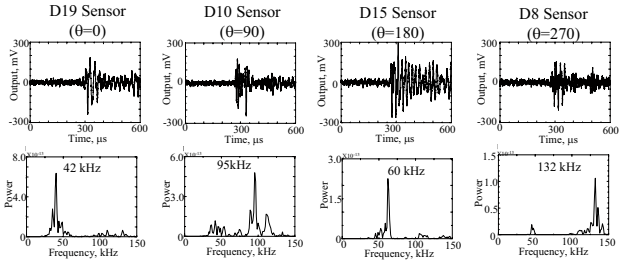

Fig.3 Waveforms and frequency spectra of AE signals detected by ITFDS

the waveforms and power spectra. Each wave shows frequency component corresponding to the resonance frequency of the element. Thus we can determine the direction of the water born P-wave at 90˚ interval.

We next monitored the P-wave at angles of 30, 45 and 60˚. These angles are noted to be between the D19 sensor (42 kHz) and D10 sensor (96 kHz). Figure 4 shows the detected waves. We observed two or three wave packets. Power spectra show two higher peaks at around 42 and 96 kHz. Using the normalized amplitude profiles of 42 and 96 kHz components of Fig.5, we can estimate the direction of the P-wave at 30˚ interval.

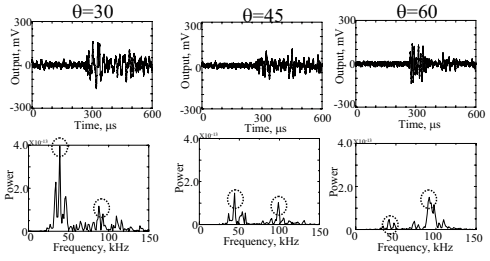

Fig.4 Waveforms and frequency spectra of water born AEs detected by ITFDS at θ = 30, 45 and 60

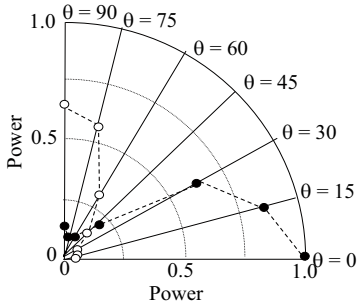

Fig.5 Amplitude profile as a function of the angle θ of ITFDS

Monitoring of Water Borne P-wave From Rust Fractures

Experimental Setup

We monitored AE signals from rust fractures using the ITFDS for 50 days. Experimental setup is shown in Fig.6. We inserted four steel plates in the four side walls of a rectangular water container with 450 mm width, 440 mm depth and 630 mm length. Four steel plates were taken from tank yard in the coastal area, and possess the natural rust produced by atmospheric corrosion. Figure 4 shows photos of sample A at being inserted in the side walls. As these samples possess the rusts on one side, the samples were inserted in the side wall using silicon rubber sealant so as the rust surface being outward of the box. Sample size, area of rust, rust thickness and corrosion method are shown in Table 1. Rust area is different among the samples, but we used them at as-received condition, since the rust tended to separate during cutting. It is noted that the thickness of the natural rust decreses in the order of Sample A(0.3 mm) →B(0.18 mm)→C(0.06 mm)→D(0.04mm). Area of the rust is approximately the same.

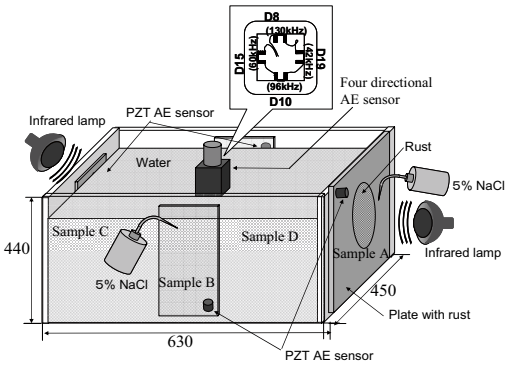

Fig.6 Experimental setup for monitoring AE from rust fracture on corroded four plates

Table 1 Specimen size, area of rust and corrosion test method

Sample	Size (mm)	Area of rust (cm^2)	Thickness of rust (mm)	Corrosion element
A	$380^{W}x370^{H}x10^{T}$	247	0.30	Mist spray(5% NaCl)+ Thermal Cycle
B	$100^{W}x240^{H}x4^{T}$	240	0.18	Mist spray(5% NaCl)
C	$80^{W}x290^{H}x6^{T}$	232	0.06	Thermal Cycle
D	$80^{W}x280^{H}x6^{T}$	224	0.04	Room atmosphere

These samples were again corroded in a non-air conditioned room using different methods in the Table 1. The sample A with the most thick rust was exposed to both thermal cycles (heating to 23 °C and natural cooling to the room temperature) and mist spraying of 5 % NaCl solution to the rust, by painting silicone grease on another portion. The sample B was mist sprayed of 5% NaCl solutions without thermal cycles. The sample C was exposed to the thermal cycles. No thermal cycle and mist spray were given to sample D. Here the thermal cycles were given by on-off of an infrared lamp for 6 hours intervals. The Mist was sprayed for 60 minutes (total spray amount 66 cc for sample A, 24 cc for sample B) at 8 hour intervals. Thus the sample A was exposed to the most severe corrosion environment and the sample D to the mildest environment. These combinations were selected as to simulate the corrosion condition which each sample was supposed to be exposured.

The container was filled with water. A trace of corrosion inhibitor was added to prevent wet corrosion of inner surface of the samples. Box type sensor was immersed into the water as the bottom of it being at 200 mm height. Experimental setup is shown in Fig.6. We also mounted PZT type AE sensor (PAC Type PICO) on the abraded portion of four samples to examine the timing and amplitude of the water borne P-wave and Lamb wave. Outputs of the PZT sensors were amplified by 40 dB, while those of the ITFDS were not amplified. AE monitoring was started on February 27, 2007 and continued to April 19 for 51 days. We simultaneously measured both the room temperature and temperature of samples A and C.

AE activities

Figure 8 shows change of room temperature and cumulative AE events counts of the ITFDS. Here one cycle of the temperature corresponds to the temperature change in one day, and the cumulative event counts mean all events from four samples, since the four sensors were connected on a single fiber in a cascade manner. We had two cold days in March 25 and April 9. We observed four fairly large step-wise increases, as indicated by four ellipses. Step-wise increases of number 2 and 3 coincide with large temperature changes, but another two (1 and 4) at higher temperatures. It is

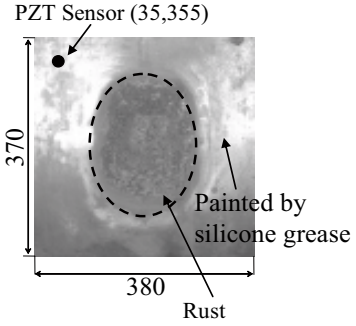

Fig.7 Sample A with rust before the corrosion test

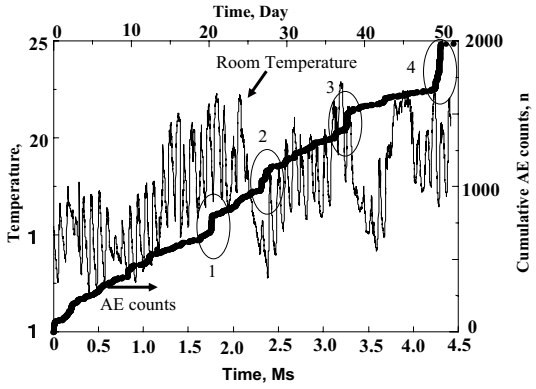

Fig.8 Change of Temperature and cumulative AE counts by optical fiber AE system

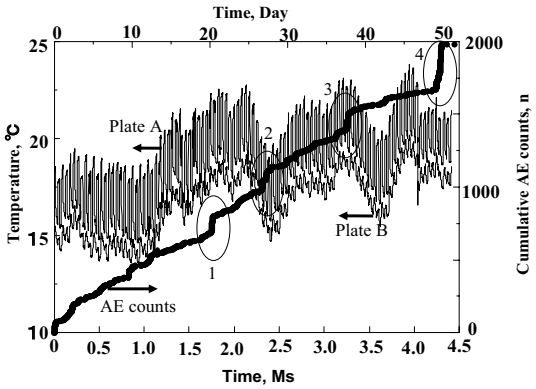

Fig.9 Change of Temperature of plate A and B and cumulative AE counts by optical fiber AE system

noteworthy that very few AE signals were emitted for approximately ten days from 38 to 47 th days.

We are keeping our opinion that the rust fractures will be accelerated by temperature change of the member. Then we studied relations between the temperature change of the samples A and B and event counts, since AE signals were supposed to be mostly generated by these samples. As shown in Fig.9, we observed a fairly good relation between the plate temperature and event counts. Stepwise increases of AE events tend to occur when the plate temperature is at high or low. Stepwise increases of No. 1, 3 and 4 occurred at higher temperature and that of No. 2 at low temperature. However, very few AE signals were emitted at 3.7 Ms (42nd day) in spite of low temperature. This appears to be due to capricious nature of grwoing rust, which often makes corrosion monitoring of tanks difficult. It is also noted that the corrosion rate can not be estimated from AE data monitored for one or two hours.

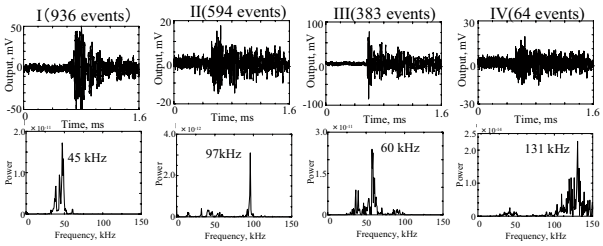

Fig.10 Waveforms and their frequency spectra detected by four optical fiber sensors

Direction of the P-wave

We next estimated the direction of the P-wave. Figure 10 shows typical examples of AE signals. Event I was classified as the AE from the sample A due to its strong frequency component at 45 kHz (D19 sensor). It counted 936 events. In the same manner, event II as from the sample B (by D10 sensor). We observe two or three wave packets in events III (D15 sensor) and IV (D8 sensor). Two peaks at 40 kHz and 60 kHz of the event III suggest simultaneous emission from the samples C and A, respectively. Two packets of the event IV suggest two AE signals from the sample D due to frequency component at around 130 kHz.

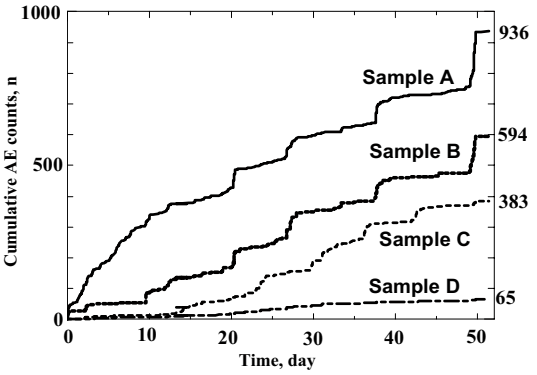

Fig.11 Cumulative AE counts from four samples

Figure 11 shows change of classified events with time. Sample A with large thick rust produced much AE signals when exposed to severe corrosion, but the sample D, exposed to mild environment, less AE signals. These are expected result, and nothing new. However, it is noted that the event count of sample C, exposed to the thermal cycle, is large.

We next compared the event counts per unit rust area. Figure 12 shows change of classified event counts per 100 cm^2 from the

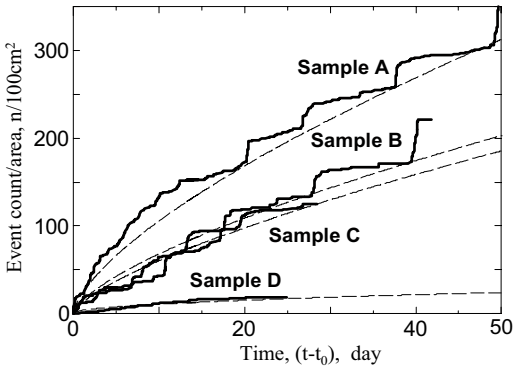

Fig.12 Change of classified event counts of AE signals from four samples

samples A,B,C and D. There observed some interesting findings. These are

1) Cumulative event counts: N increase with time:t according to the parabolic law, i.e., $N=N_o(t-t_o)^n$, where $n<1$. This law is common to high temperature oxidation of metals covered by protective oxide film. Small N_o and n indicate protective film. Steps in parabolic oxidation curve indicate the rapid oxidation due to partial breakdown of the film. These correspond to the stepwise increase of AE signals due to fractures of the rust.
2) Incubation time:t_o becomes longer for the samples exposed to mild corrosion condition.
3) There are slight time lags in the timing of steps for samples A, B and C, suggesting that the AE activity changes depending on the rust history and corrosion environment. Step height of samples A and B with thicker rust are larger than that of sample C.
4) In spite of non corrosive environment, sample C shows higher emission rate.

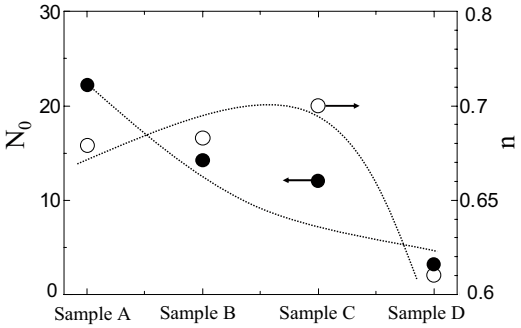

Fig.13 Parameter: N_0 and n estimated for four samples

We next determined two parameters: N_o and n by curve fitting of the time-shifted data. Here the parameters were decided so as the parabolic curves pass through the bottom of the steps, as shown in Fig. 12. Due to the limited data for only 50 days, correct determination was impossible, but tentatively estimated as shown in Fig.13. The parameter N_0 increases in the order of samples D->C->B->A, indicating corrosiveness and rust nature. The parameter: n presents the role of rust on the corrosion rate. Here it is noted that the rust plays two roles. One is protection of the base metal as a diffusion barrier of water and oxygen. Another is acceleration effect of corrosion by lowering the acidity of impregnated water. The latter is enhanced by chloride ions. It is note worth that the sample A, with thicker rust and exposed to severe corrosion condition, shows n=0.68, almost the same values for the samples B (0.685) and C(0.7). This suggests the rust on the sample A is playing a protection effect. Higher n of the sample C is, rather, noted.

In order to study relationship between these parameters and corrosion rate of the substrate steel, we measured the growth rate of the rust under four corrosion conditions. Bare steel plates were exposed to four corrosion condition, and rust thickness was measured by optical microscope after 7, 15 and 25 days. Photograph of sample B after 15 days test is shown in Fig.14. Growth rate of the rust by the condition given to the sample A is estimated as 12 μ m/10 days (432 μ m/year). Those by the environments to samples B and C are 5 μm/10days (180 μm/year) and 3 μ m/10 days (108 μ m/year), respectively. We observed many cracks in the rust produced by 15 days corrosion tests given to the samples A and B. The rust suffered cracks by its

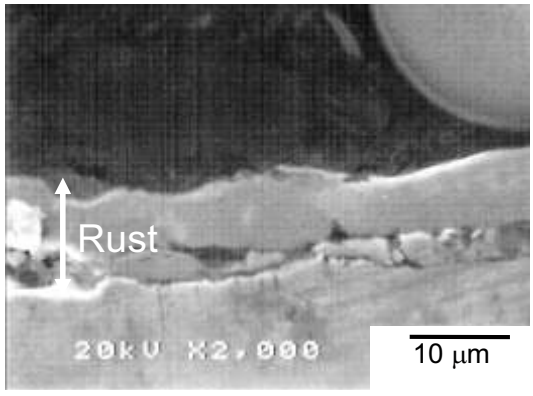

Fig.14 Cross section of bare steel plate exposed to mist spray corrosion after 15 days

volumetric expansion after 15 days. The parameter: N_0, i,e; AE counts after one day, is closely related to the growth rate of the rust. It is, however, absolutely impossible for the corrodent to penetrate into the substrate through the thick rust and cause corrosion of the substrate in one day. Then we studied where AE sources are.

Figure 15 shows transverse SEM of the sample B. Higher concentration of Fe by EPMA are shown by dotted white lines. We observed a number of steel pieces in the rust, in addition to iron oxides (Fe_2O_3 and Fe_3O_4) . More interesting is a number of cracks near the steel pieces. We observed cracks starting from the steel pieces in the rust. EPMA analysis of the Sample A showed the same features.

In order to study the AE activity of the rust itself, we moniotrred AEs from the rust pieces immsered in a slightly acidic solution (sulfuric acid solution of pH= 3.0 at 27 C) . AEs were moniotred by PZT sensor mounted on the 300 ml glass beaker. Three pieces of fallen rusts in tank yard (Fig.16) were tetsed for 20 hours. All specimens are found to be composed of multi layers and contain metallic pieces.

Figure 17 shows an example of AE signal from rust A. Burst-type signal designates the water born P-wave produced by the rust fracture due to corrosion of metallic pieces in the rust. Figure 18 shows change of AE events with time for three rust pieces. AE activity chnages depending on the rust nature.

We found that AE activity rapidly increased when the piece was broken, as seen in the step-wise increase of AE for the piece C. This indicates that the ruts acts as a diffusion barrier to freash water with dissolved oxygen.

Above data strongly suggests that the AE sources are not the fracture of the rust produced by corrosion of the substrate steel, but the rust fracture due to the corrosion of steel pieces included in the rust. There appears to be no relation between the corrosion rate of substrate steel and AE events.

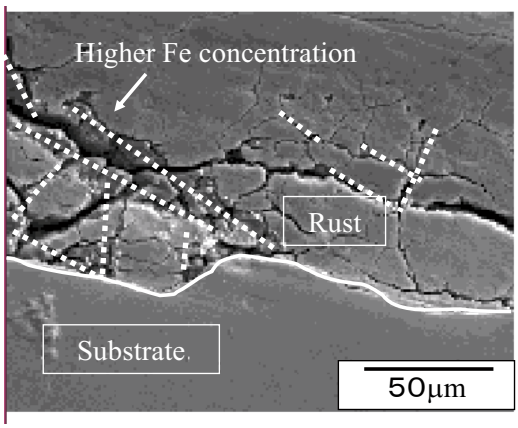

Fig.15 Transverse SEM of rust on sample B exposed to corrosion acceleration test

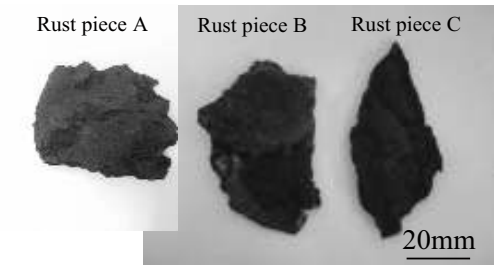

Fig.16 Three rust pieces to monitor liquid borne AE

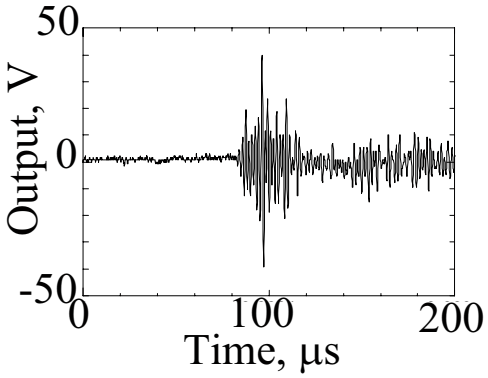

Fig.17 Waveform detected by PZT sensor mounted on side wall of a glass beaker

Conclusion

We developed a four directional AE system and monitored liquid-borne AE signals from four corroded plates which were exposed to different corrosion environment.

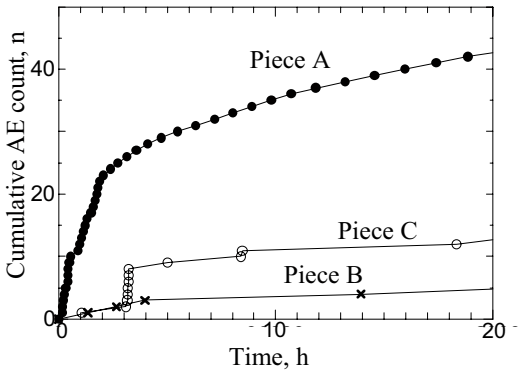

Fig.18 Cumulative AE counts from three rust pieces

1) We developed immersion type four directional sensor by utilizing optical fiber AE system. It detected AEs from four directions simultaneously. Source direction can be defied by frequency characteristics of four sensors.
2) The sensor monitored the water-borne P-wave from rust fracture. Direction of the P-waves was successfully discriminated using the resonance frequencies of four sensors.
3) We observed good relations between AE activity and plate temperature. Stepwise increases of AE events tend to occur when the plate temperature is at higher or lower .
3) AE events increased with time according to the parabolic law: $N=N_o(t-t_o)^n$, suggesting protective nature of the rust.
4) AE sources in the corroded plates were supposed to be the rust fractures due to corrosion of steel pieces included in the rust , but not the corrosion of the substrate steel.

References

1. *Corrosion Center News*, 29, Japan Society of Corrosion Engineering, 2004
2. H.Cho,R.Arai and M.Takemoto, J.Acoustic Emission,23, 2005,72-80
3. T.Matsuo, H.Cho and M.Takemoto, *Progress in Acoustic Emission XIII*, IAES-18, 2006, 311-318